Analysis of the thermal recovery of HTS cables after an overcurrent fault

J A Demko[1], R. C. Duckworth[2], G. Churu[1], and W. Hasssenzahl[3]

[1]LeTourneau University, 2100 South Mobberly Avenue, Longview, TX 75607 USA
[2]Oak Ridge National Laboratory, One Bethel Valley Road, Oak Ridge, TN, 37831 USA
[3]Advanced Energy Analysis, 1020 Rose Ave., Piedmont, CA, 96411-4345 USA

Abstract. High temperature superconducting (HTS) power transmission cables are cooled to operating temperatures typically below 80 K using liquid nitrogen or gaseous helium. HTS cables are being considered for applications including connecting substations to allow transformers to share load, and long-distance, low-loss electrical power transmission. A valuable feature of some HTS cables is that they can limit short-circuit fault currents, which can be more than ten times the maximum operating current of a cable. When a fault occurs, the cable current exceeds the critical current of the HTS and may raise the temperature above the allowable operating point so the conductor must be cooled down before returning to service. The recovery process of an HTS power transmission cable depends on several factors including the cooling scheme (counterflow or parallel flow), the way in which the refrigeration system's performance varies with load and temperature, the energy deposited during the fault, and the operating temperature margin. This study investigates thermal recovery after a fault for some HTS cable system configurations and operating conditions.

1 Introduction

High temperature superconducting (HTS) cables offer benefits in situations such as connecting substations, controlling faults, distributing power through high-congestion areas, and transmitting DC power over long distances. Demonstration projects of different HTS cables in the electrical grid provide information to assess their performance and identify issues related to maintaining their temperature. These issues have been assessed across a broad operational spectrum with projects with running lengths around 1 km [1-3], voltages from 15 kV distribution level to transmission levels above 115 kV [4-6], and urban installations with highly constrained right of ways and footprints [1, 7-8]. Here we address the issue of fault recovery of an HTS cable system in short to medium length, three-phase, AC triaxial cables.

Fault currents are an operational certainty that every HTS cable installation must mitigate when installed in the grid. Faults occur in power delivery systems to varying degrees as a result of natural disasters, equipment failure, and accidents. Through faults are low current faults on the order of three to five times the maximum operating current and multiple cycles that typically will not trip the cable system off-line nor do they deposit a sufficient energy to require that the cable stay off-line for any period of time. High-current faults occur less frequently and involve currents that can exceed twenty times the maximum operating current of the power system When a high-current fault occurs, the HTS material transitions to a normal, resistive, conductor and generates a sufficient energy to heat up the cable. The Southwire American Electric Power (AEP) Bixby substation demonstration was a 200-meter-long parallel flow cooled cable which connected two transformers within a substation [3]. The cable is a

triaxial design where the three current carrying phases are wound concentrically as shown in Figure 1. In preparation for the cable design, it was determined through analysis and testing that an overcurrent fault would deposit around 6 kJ per meter. During routine operation, the cable withstood several faults without interruption of service. The Hydra project is a proposed project with the goal of installing a triaxial fault current limiting HTS cable in in the New York City power grid that would be approximately 300 meters long. It was designed to carry 96 MVA at 13.8 kV at a current of 4 kA. The design fault current is 40 kA and it is to attenuate the maximum current by 17% [8]. Proof-of-principle was demonstrated at Oak Ridge National Laboratory tested a 25-meter prototype of the Hydra project cable [9]. For these concepts as well as others mentioned earlier especially those that push the boundaries with respect to installation length, the design of a successful HTS installation accounts for these faults in the context of cooling provided.

Two basic approaches are possible for cooling an HTS cable to operating temperature and maintaining this temperature during operation. The first (A) is to provide a source of liquid nitrogen and to pump the fluid through the cable. The liquid nitrogen is trucked to the installation where it is transferred to a storage cryostat for use as needed to maintain cable operation. The second (B) is to install a refrigeration system to extract heat from the cable by forced flow of a fluid through the cable. In either of these cases, there are two sub-categories. First, (i) the fluid can be forced along the cable from one end and then either discard it at the other end or return it in a separate, thermally insulated, conduit. Second, (ii) the fluid can be forced along the cable in one direction and then be return to the sending end of the cable via a path that is in limited thermal contact with the outgoing fluid. This approach is shown in Figure 1. To choose the type of cooling system to use for a given installation, the system designer must assess factors such as include initial capital cost, operating cost, efficiency, simplicity, reliability, and expected period of service. One aspect of this reliability is the response of the cooling system to fault currents.

Previous work investigated different aspects of an HTS cable response to a fault [10-14]. The radial thermal response time of a triaxial cable was calculated to be on the order of 15 to 30 seconds [10]. Other investigators modelled the voltage, current, temperature characteristics of the HTS conductor [12,13]. Certain aspects of the cryogenics pertaining to the LIPA HTS cable response to a 69 kA fault can be found in [5,13].

2 Computational model and assumptions

The calculations were performed assuming a one-dimensional thermal model of a triaxial HTS cable. I.e., the cable is axially segmented, and each segment has three characteristic temperatures: the temperature of the nitrogen inside the former, the temperature of the body of the cable, and the temperature of the nitrogen in the outer annular space. Details regarding simulating a counterflow cooled superconducting cable can be found in [15,16]. Heat transfer occurs at the boundaries between the cable body and the two nitrogen streams. The operating pressure of the input liquid nitrogen is high enough such that the maximum temperature in all cases will not produce gaseous nitrogen. A typical build for the cable is provided in Table 1. The inner layer of conductor is wound over a former that maintains a circular shape for the entire cable. A shield layer is provided as an outside layer of the cable. Its purpose is to carry any current imbalance between the three phases. The current imbalance is assumed to be zero for this study so there will be no resistive heating in the shield conductor. The dielectric thickness is between the layers similar to a 13.8 kV class cable. For higher voltages, a thicker dielectric layer between the phases would be necessary. The critical currents, I_c, of the three phases at 77 K are prescribed as 6.9 kA, 7.6 kA and 7.7 kA for the three phases starting with the innermost phase. The I_c is scaled linearly with temperature assuming that I_c=0 at 104 K.

The model used the counterflow cooling arrangement and the mass flow is assumed to be constant along the length of the cable. After leaving the refrigeration unit, the liquid nitrogen enters and then flows through the former until it reaches the far end of the cable. It then cools the far end termination before returning via the annular space between the outside of the cable and the inner wall of the cryostat. Finally, it cools the supply end termination before returning to the refrigerator. In this study both end terminations are rated for 3000 A per phase and provide connections for three phases and a ground. The

estimated heat load is 1120 W per termination. The termination heat loads are assumed constant but would vary with current due to resistive heating in the current leads.

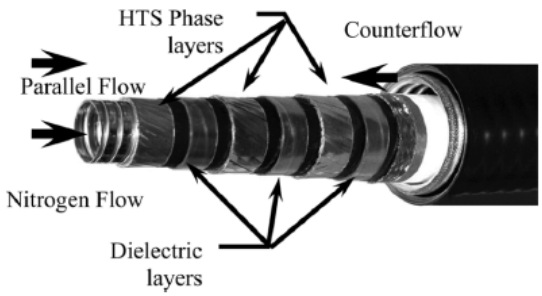

Figure 1. Basic construction of a triaxial HTS cable**.**

Table 1. Typical layers in a generic Triaxial HTS cable.

Layer	Diameter (mm)
Former	50
Former OD	53.2
Bedding	54
HTS Phase 1	54.9
Dielectric	59.7
HTS Phase 2	60.7
Dielectric	65.5
HTS Phase 3	66.5
Dielectric	71.3
Copper shield or neutral	79.5
Inner wall of cryostat	98

2.1 Computational Differential equations of the energy balance

Recovery after a fault is a thermal problem dealing with the energy removal and cool down of a cable to a suitable temperature for placing it back in service. This is mainly an issue that is determined by the refrigeration system and the total heat load. Thus, a complicated model of the system, for example including radial heat transfer within the cable and establishing a detailed finite element model will have little effect on the recovery time. However, it would increase the calculation time considerably. Thus, a 1-D model is chosen for this analysis.

The one-dimensional energy balance equations for the HTS power-transmission cable system are solved numerically to determine the temperature distributions in the nitrogen cooling streams and along the HTS cable. In this study, T_{cab} represents the temperature of the tri-axial cable. It is used to approximately determine the axial temperature gradient of the cable in the energy balance discussed below. For the HTS cable, the one-dimensional energy balance equation can be written as in equation (1), where z is the coordinate direction along the cable axis, k_{cable} is the cable axial thermal conductivity, A is the cable cross-sectional area, and P'_{AC} is the ac loss per unit length.

$$\frac{\partial T_{cab}}{\partial t} = \frac{\partial}{\partial z}\left(k_{cable} A \frac{\partial T_{cab}}{\partial z}\right) + P'_{AC} - \sum_j Q'_{conv,j} \tag{1}$$

Two convection heat-transfer terms, $Q'_{conv,j}$ represent convection to the nitrogen flow in the outer annular region and to that in the cryostat former, where j represents the two streams. Additional energy-balance equations for the liquid streams and are given by equation (2), where $i(T,P)$ is the enthalpy of the fluid stream that is a function of temperature and pressure, where w_{LN2} is the liquid nitrogen mass flow.

$$\frac{\partial T_{LN2,j}}{\partial t} = w_{LN2} \frac{\partial i(T_{LN2,j}, P_j)_{v,j}}{\partial z} + \sum_j Q'_{conv,j} \tag{2}$$

The pressure drop in the liquid nitrogen is determined during the iteration process from the momentum equation. The variables f and D_{hyd} are the friction factor, and the hydraulic diameter of the flow path respectively; they are fixed for each run. The variables $p, V, and\ \rho$ are the pressure, velocity and density of the nitrogen respectively. Liquid nitrogen properties were determined using REFPROP [17].

$$dp + \rho V dV + f\frac{\rho V^2\ dz}{2\ D_{hyd}} = 0 \quad (3)$$

Heat input to the cable system has been discussed in detail in many other cable papers [4]. These heat sources include the cryostat heat load, ac loss within the conductors, dielectric loss, and the termination heat loads at each end of the cable. The cryostat heat load is assumed to be a constant 1.5 W/m along the length of the cable. AC losses have been determined using the mono-block model. The initial starting solution prior to a fault is assumed to be a steady state operation at full current.

Fault currents of 10 to 40 times the nominal current may occur. In this study the cable limits the overcurrent to 30 times nominal. Testing performed for the AEP cable system measured energy deposited during a fault at around 6.2 kJ per meter. For this study, the energy deposited during a fault is 1.2 MJ for a 250-meter cable and 10 MJ for the 1000-meter-long cable.

2.2 Refrigerator performance model

In this simulation of a thermal response and recovery from fault of an HTS cable, the refrigerator performance plays a critical role. The refrigeration system for an HTS cable application is designed for a maximum load at the highest operating current and includes some margin due to uncertainty in the estimated loads. The calculated baseline heat load, $Q_{baseline}$, is determined from a steady state calculation of the total thermal loads at the full operating current. The refrigerator capacity, Q_{Refr}, is equal to the baseline plus some assumed margin. These values are shown in Table 2.

In general, there are two refrigerator design characteristics that can affect the coolant supply temperature. The first is the size of the heat exchanger with which the refrigerator cools the return stream. It is assumed that the heat exchanger is large enough that its performance does not affect the temperature of the cooling stream. This can be explained by the heat exchanger relation:

$$Q = AU\Delta T_{log-mean} \quad (4)$$

The heat transferred across the heat exchanger is modelled as a function of the surface area, A, the overall heat transfer coefficient, U, and the log mean temperature difference (LMTD), $\Delta T_{log-mean}$. The LMTD is determined from the temperatures of the return stream, and the temperatures produced in the refrigerator. In this study, it is assumed that the overall heat transfer coefficient is constant, and that the surface area is constant. Both parameters are assumed to be sufficiently large so that only the temperatures produced by the refrigerator will increase for excessive heat loads greater than the capacity of the unit.

When the heat load is significantly higher, the refrigeration system responds by providing higher temperatures to balance the higher load. In this study, the scaling of the supply temperature assumes a constant input power to the refrigerator at the maximum capacity for all heat loads above the maximum baseline heat load, as would be experienced during a large fault. When the heat load is below the refrigerator capacity, the supply temperature is a constant 72 K. This assumes that the power supplied to the refrigerator unit can be adjusted to the load so that the temperature of the coolant supply remains constant.

The Carnot scaling is accomplished assuming that for loads above the refrigerator rated capacity, the input Carnot power remains constant:

$$P_{Carnot} = Q_{Refr}\frac{(T_H - T_L)}{T_L} \quad (5)$$

Where the ambient temperature is $T_H = 300K$ and the refrigeration temperature is $T_L = 72\ K$. When the heat load of the HTS cable system, Q_{Sys}, becomes greater than the rated capacity of the cooling system Q_{Refr}, the refrigerator temperature, $T_L{}'$ can be solved using a similar Carnot performance in terms of the system heat load as:

$$T_L{}' = \frac{Q_{Sys}T_H}{(P_{Carnot} + Q_{Sys})} \quad (6)$$

This is shown graphically for several different heat loads in Figure 2. The constant inlet temperature model corresponds to an unlimited refrigerator cooling capacity.

2.3 Boundary conditions and solution method

The boundary conditions are that there is no heat transfer axially from the ends, and the that the cable surface is cooled by convection heat transfer to the liquid nitrogen. The inlet flow temperature to the former is determined by refrigerator performance. The differential equations are integrated in time following the numerical method of lines approach [18] and the ordinary differential equation (ode) solver package DLSODES from odepack [19].

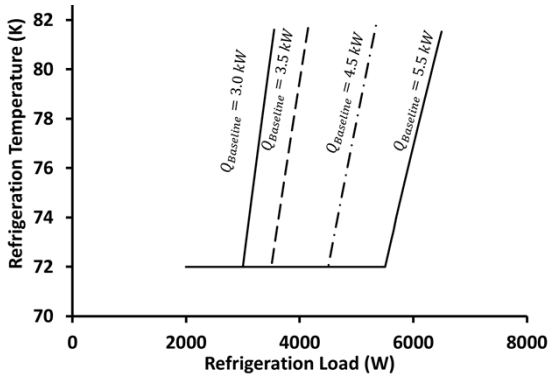

Figure 2. Carnot scaling of refrigerator temperature as heat load increases above baseline.

Table 2. Baseline refrigeration load and refrigeration system parameters

Case	$Q_{baseline}$ (W)	Q_{Refr} (W)
250-meter counterflow	2884	3000
1000-meter counterflow	4649	5000 and 7500

3 Simulation results for the 250-meter cable

The inlet conditions of the liquid nitrogen are provided in Table 3. Prior to the fault an ac current is 3 kA. The ac loss causes the temperature profiles for the nitrogen in the former and annulus and for the solid cable shown in Figure 3. The jump in temperature at far end of the cable is caused by the termination heat load. Figure 4 shows the same temperatures just after the fault. Since the fault occurs over 0.2 seconds, there is insufficient time for the liquid nitrogen streams to respond to the temperature rise of the cable.

Table 3. Flow parameters for the 250-meter case.

Inlet pressure (bar)	Inlet Temperature (K)	Flow (kg/s)	Former flow velocity (m/s)	Annulus flow velocity (m/s)	Pressure drop (bar)
19	72	0.6	0.366	0.302	0.669

The supply and return liquid nitrogen temperatures are compared in Figure 5 for the unlimited refrigeration and the limited refrigeration cases. (Note that ac power starts at -5000 sec.) The calculated heat loads are given in Figure 6. As expected, the return temperatures are lower for all times when the supply temperature remains constant at 72 K. The response of the return liquid nitrogen temperature follows the response of the supply temperature. Since the focus of this study is the recovery of the cable for placement back into service after a fault, these results show a significant difference in the recovery time if the refrigerator is unable to maintain a low temperature supply.

The heat loads calculated in Figure 6 show that with unlimited refrigeration the fault causes a roughly 50% increase in the heat load. This indicates that for the quickest recovery from a fault of the prescribed magnitude would require 4.5 kW at 72 K instead of the 3 kW which was applied in this model. The heat load for the constant current case falls below the initial value because after the fault, the current is assumed to be zero so there is no ac loss in the cable. Bases on the heat load, recovery would appear to be around 5000 seconds for the unlimited refrigeration case, but significantly longer for the limited refrigerator case.

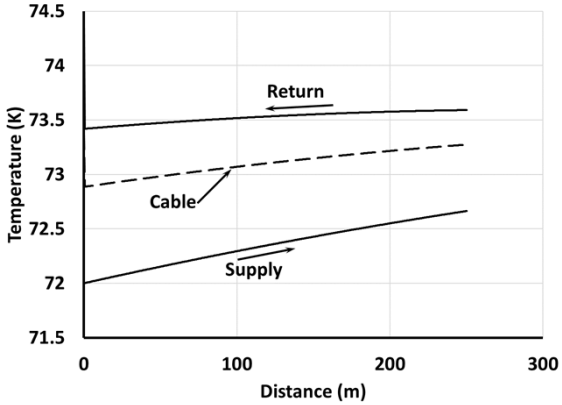

Figure 3. Steady state temperature distribution at full current prior to fault for 250-meter cable.

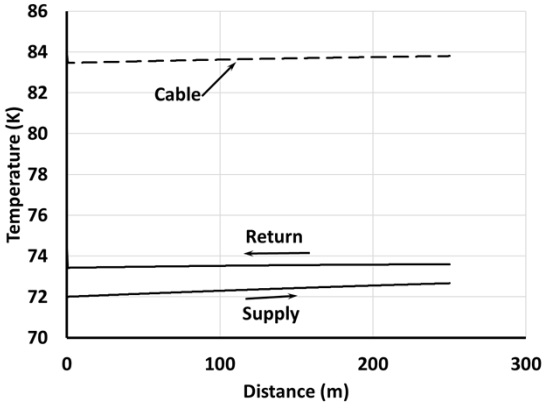

Figure 4. Temperature distribution after the fault for 250-meter long HTS cable.

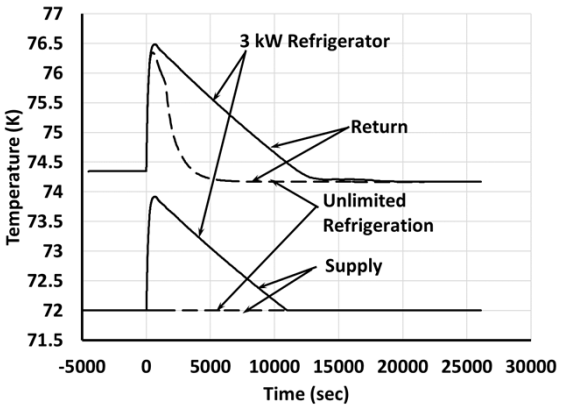

Figure 5. Liquid nitrogen temperature for supply and return flow after a fault.

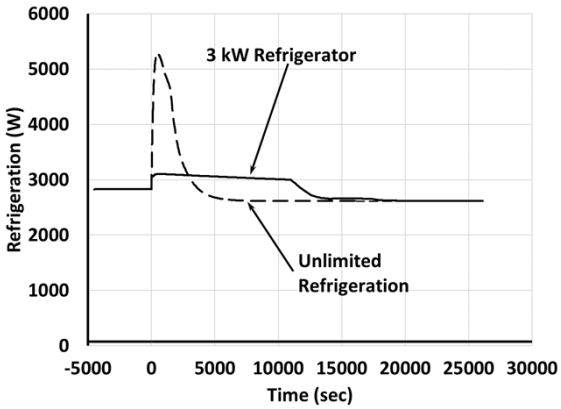

Figure 6. Cryogenic system heat removal after a fault.

4 Results for 1000-meter cable

For the 1000-meter cable the flow parameters are provided in Table 4. The temperature distributions before the fault and just after the fault are shown for the 1000-meter cable in Figures 7 and 8. Applying a 10 MJ fault the cable temperatures are slightly higher than for the 250-meter case presented here.

Table 4. Flow parameters for the 1000-meter case.

Inlet pressure (bar)	Inlet Temperature (K)	Flow (kg/s)	Former flow velocity (m/s)	Annulus flow velocity (m/s)	Pressure drop (bar)
19	72	1.75	1.06	0.882	6.26

The transient response of the nitrogen stream temperatures are compared in Figure 9. The heat load for the unlimited refrigeration case, shown in Figure 10, goes from the steady state value of 4.7 kW to over 13 kW. This more than twice the baseline capacity of the refrigerator used in this model. The unlimited refrigeration case recovered after around 8000 seconds indicating an effect due to the longer length of the cable. With the 5 kW refrigerator, recovery based on heat load is aat around 21000 seconds. Increasing the refrigerator capacity to 7.5 kW reduced the recovery time to around 1000 seconds.

The average cable temperatures are extremely high, and it may be that the conductor temperature is higher inside the cable. There are three possibilities for any nitrogen inside the cable. First, the nitrogen vaporizes and expands inside the cable. This is unlikely from experience since that would cause the cable to deform. This was not observed in the Hydra project cable testing [5]. A second possibility is

that liquid that is vaporized vents from the cable. If this occurs, the cooling stream outside the cable is much colder than the vapor and would immediately collapse any vapor that made its way into the stream. The third possibility is that the liquid nitrogen trapped remains trapped inside the very small voids and the pressure is contained at high levels in the voids.

5 Summary, Conclusions and Recommendations for Future Work

A simulation of the recovery of an HTS cable has been performed assuming a generic refrigerator model. The cable has recovered when the temperature of the cable cools down to the values before the fault occurred. Using a sufficiently large refrigerator, such that the coolant supply temperature remains constant will provide a significantly shorter time to recovery than if an increase in temperature of only a few Kelvins takes place.

One recommendation is to use the thermal characteristics of the cable materials to develop a two-dimensional model including radial heat transfer across the cable. This would allow a more detailed assessment of the cable internal temperature. A simplified version of this technique was used by two of the authors in an assessment of HTS DC cables.

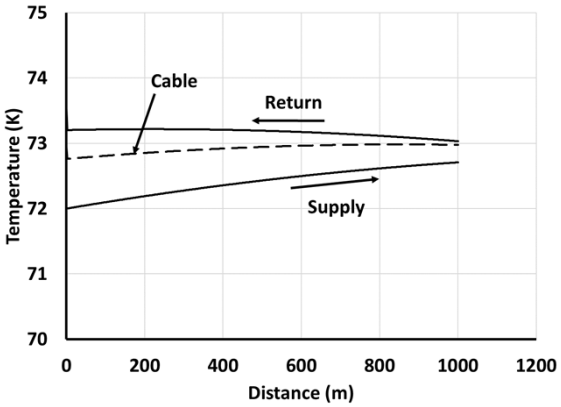

Figure 7. Steady state temperature and pressure distribution at full current prior to fault for 1000-meter long HTS cable.

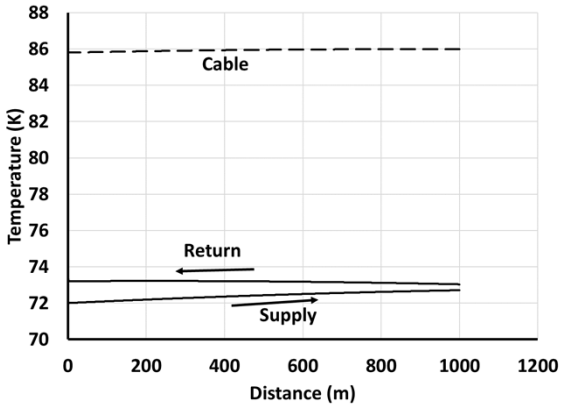

Figure 8. Temperature distribution at the end of the fault for 1000-meter long HTS cable.

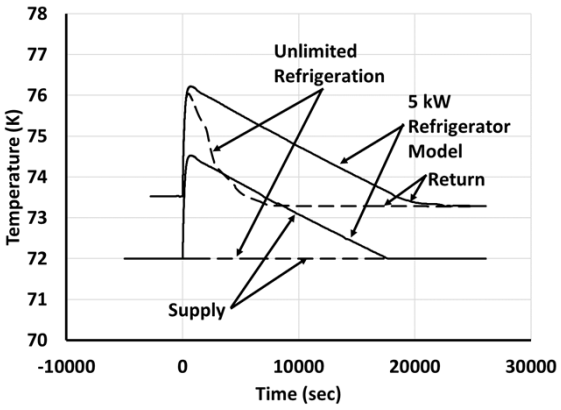

Figure 9. Liquid nitrogen temperature responses after a fault for the 1-km cable.

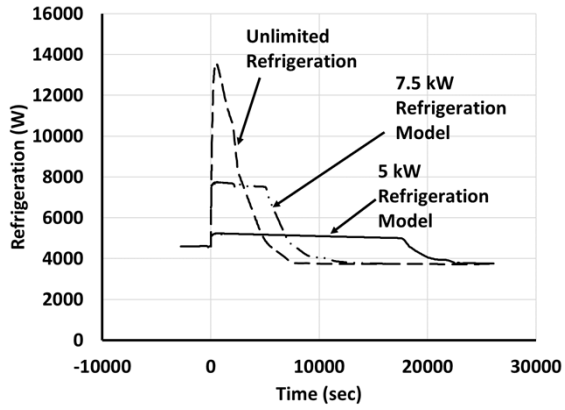

Figure 10. Cryogenic system heat load response after a fault in the 1-km cable.

6 References

[1] Stemmle M, Merschel F, Noe M, and Hobl, A 2013 AmpaCity – Installation of advanced superconducting 10 kV system in city center replaces conventional 110 kV cables *Proc. 2013 IEEE Intl. Conf. Appl. Supercond. Electro. Dev* 323-326

[2] Lee S R, Lee J J, Yoon J, Kang W, and Hur J 2016 Impact of 154 kV HTS cable to protection

systems of the power grid in South Korea *IEEE Trans. Appl. Supercond.* 26 5402404.
[3] Demko J A, Sauers I, James D R, Gouge M J, Lindsay D, Roden M, Tolbert J, Willen D, Traeholt C, and Nielsen C T 2007 Triaxial HTS cable for the AEP Bixby project *IEEE Trans. Appl. Supercond.* 17 pp. 2047-2050
[4] Maguire J F, Yuan J, Romanosky W, Schmidt F, Soika R, Bratt S, Durand F, King C, McNamara J, and Welsh T E 2011 Progress and status of a 2G HTS power cable to be installed in the Long Island power authority (LIPA) grid *IEEE Trans. Appl. Supercond.* 21 961
[5] Weber C S, Lee R, Ringo S, Masuda T, Yumura H and Moscovic J 2007 Testing and demonstration results of the 350 m long HTS cable system installed in Albany, NY *IEEE Trans. Appl. Supercond*. 17 2038–42
[6] Maruyama O, 2015 Results of Japan's first in-grid operation of 200-MVA superconducting cable system *IEEE Trans. Appl. Supercond.* 25 5401606
[7] Zong X, Wei D, Han Y, and Tang T 2016 Development of 35 kV 2000 A cd HTS cable demonstration project *IEEE Trans. Appl. Supercond.* 26 5403404
[8] Maguire J, Folts D, Yuan J, Henderson N, Lindsay D, Knoll D, Rey C, Duckworth R, Gouge M, Wolff Z, and Kurtz S 2010 Status and progress of a fault current limiting HTS cable to be installed in the con edison grid *AIP Conf. Proc.* 1218, 445
[9] Rey C M, Duckworth R C, Demko J A, James D R, and Gouge M J 2010 Test results of a 25-m prototype fault current limiting HTS cable for project hydra, *AIP Conf. Proc.* 1218 453
[10] Hu N, Toda M, Watanbe T, Tsuda M, and Hamajima T 2011 Recovery time analysis in a tri-axial HTS cable after an over-current fault *Physica C* 471 1295
[11] Kojima H, Osawa T, and Hayakawa N 2015 Fault current limitation coordination in power transmission system with superconducting fault current limiting cables (SFCLC) *IEEE Trans. Appl. Supercond.* 25 2392251
[12] Su R, Shi J, Yan S, Li P, Wan W, Hu Z, Zhang B, Tang Y, Ren L, Li J, and Xu Y 2019 Numerical model of HTS cable and its electric-thermal properties *IEEE Trans. Appl. Supercond.* 29 2901874
[13] Yuan J, Maguire J, Allais A, and Schmidt F 2005 A cool-down and fault study of a long-length HTS power cable *AIP Conf. Proc.* 823 782
[14] Hu N, Cao K, Wang D, Song M, Miyagi D, Tsuda M, and Hamajima T 2013 Transient thermal analysis of a tri-axial HTS cable on fault current conditions *Physica C* 494 276
[15] J. A. Demko, J. W. Lue, M. J. Gouge, J. P. Stovall, Z. Butterworth, U. Sinha, and R. L. Hughey, "Practical AC loss and thermal considerations for HTS power transmission cable systems," IEEE Trans. Appl. Supercon., vol. 11, pp. 1789–1792, March 2001.
[16] G. H. Morgan and J. E. Jensen, "Counter-flow cooling of a transmission line by supercritical helium," Cryogenics, pp. 259-267, May 1977.
[17] Lemmon, E.W., Huber, M.L., McLinden, M.O., NIST Standard Reference Database 23: Reference Fluid Thermodynamic and Transport Properties-REFPROP, Version 9.1, National Institute of Standards and Technology, Standard Reference Data Program, Gaithersburg, 2013.
[18] William Schiesser, "The Numerical Method of Lines: Integration of Partial Differential Equations, Academic Press, Inc., 1991
[19] http://netlib.org/odepack/index.html, Last accessed June 6, 2019

Acknowledgments
We would like to thank LeTourneau University School of Engineering and Engineering Technology for their generous support of this research effort. This manuscript has been authored in part by UT-Battelle, LLC, under contract DE-AC05-00OR22725 with the US Department of Energy (DOE). The US Government retains and the publisher, by accepting the article for publication, acknowledges that the US Government retains a nonexclusive, paid-up, irrevocable, worldwide license to publish or reproduce the published form of this manuscript, or allow others to do so, for US government purposes. DOE will provide public access to these results of federally sponsored research in accordance with the DOE Public Access Plan (http://energy.gov/downloads/doe-public-access-plan).